17th World Conference on Earthquake Engineering, 17WCEE
Sendai, Japan - September 13th to 18th 2020
Paper N° C004131
Registration Code: S- A01045

DEVELOPMENT OF A NEW JOINT SYTEM FOR CLT PANELS

M. Maeda [1], K. Endo [2], A. Ogasawara [3], A.G. Aljuhmani [4], A.V. Shegay[5]

[1] *Professor, Graduate School of Engineering, Tohoku University, maeda@archi.tohoku.ac.jp*
[2] *Structural Engineer, Shimizu Corporation, k-endo@shimz.co.jp*
[3] *Graduate Student, Graduate School of Engineering, Tohoku University, ogasawara@rcl.archi.tohoku.ac.jp*
[4] *Graduate student, Graduate School of Engineering, Tohoku University, Japan, aljehmani@rcl.archi.tohoku.ac.jp*
[5] *Researcher, Graduate School of Engineering, Tohoku University, ashegay@rcl.archi.tohoku.ac.jp*

Abstract

Timber products are being increasingly utilized in mid- to high-rise buildings in Japan as it is a sustainable and eco-friendly material. Cross laminated timber (CLT) is one possible candidate for wide use in construction because of its high strength and stiffness characteristics. However, the development of effective seismic connections between timber elements is an ongoing challenge in timber construction. The main objective of this research is to develop a new structural joint system between CLT panels that has high shear, tensile strength and stiffness characteristics. The proposed joint consists two steel plates placed on both surfaces over the joints of adjacent CLT panels, and held in place using steel drift pins and high tension bolts going through the panel. Diagonal tension and compression forces in the pins resist the shear force generated between CLT panels during lateral loading.

In this research, a tension test of single drift pin embedded in CLT was conducted to understand the different failure mechanisms, strength and ductility characteristics. Test parameters were drift pin diameter, edge distance of the drift pins and loading direction relative to fiber direction of exterior lamina layer of the CLT panel. Findings from monotonic loading tests are: (1) failure mode is governed by the ratio of edge length, L_n, to drift pin diameter, ϕ; (2) brittle shear failure of CLT along the fiber of exterior lamina was observed at $L_n/\phi<2.5$, while ductile compression failure occurred when $L_n/\phi>2.5$; (3) strength of single pin embedded in the CLT could be evaluated using material strengths of CLT and component dimensions; and (4) the angle of loading direction to fiber direction did not affect failure mode and strength.

Next, a full scale joint element test was performed under reversed cyclic load. Test parameters were diameter of drift pins, L_n/ϕ and steel plate geometry. The joint successfully resisted shear forces between CLT panels and maximum strength could be predicted based on the results of a single pin pull out test. A narrow angle θ between the panel edge and the direction of the diagonal compression induced in the pin resulted in higher stiffness and strength characteristics of the joint. Failure mode, stiffness and strength can be controlled by careful selection of the pin diameter ϕ, edge length L_n and angle θ.

Finally, half scale CLT panel wall assemblies were tested under reversed horizontal load. Test parameters were the effectiveness of the proposed joint system to unify two panels to work as one and the use of notched steel plates to induce a steel plate failure mode. A wall specimen with two CLT panels connected by the proposed joint exhibited very similar behavior with the specimen of the same dimension but a single CLT panel unit without joints. No significant difference was found in stiffness, ultimate strength and deformation capacity. It was shown that the proposed joint system is an effective joint system for CLT panels for earthquake demands in middle to high-rise CLT building.

Keywords: CLT (Cross laminated timber), Joint, Seismic Design, cantilever walls, drift pins.

1. Introduction

In the coming years, wider application of forest resource-based materials to building construction will contribute to carbon reduction and sustainable development in the building construction field. Cross laminated timber (CLT) is an effective timber construction material because it is easy to handle in construction sites and can be designed to provide high strength and stiffness capacity to structures. Its use as an effective construction material to replace conventional structural materials, such as reinforced concrete or steel, is expanding. For these reasons, the Japanese government is promoting and encouraging to use CLT panels for public buildings through construction subsidies. In 2016, a building code for CLT panel structures was issued by the Ministry of Land, Infrastructure and Transport, which accelerated CLT design and construction.

As seismic design is critical for buildings in Japan, CLT panels and the CLT panel connections must be designed to carry both flexural and shear demands. Figure 1(a) shows the general connection layout used in CLT panel walls. Vertical anchor bolts are installed at four corners to transfer tension forces to the floor slab and steel plates and nails are attached at top and bottom ends to carry the shear force demands. These connections require a large number of anchor bolts and shear plates. A disadvantage of CLT panels is the narrow panel width (typically 1.2 m in Miyagi prefecture, Japan) as constrained by road transportation logistics as well as limited by fabrication equipment capacity. As a result, a large number of connections are required inside a structure utilizing CLT panels, and subsequently the cost of construction is high.

If narrow width CLT panels can be connected together and act as a single large panel to resist shear forces and provide equivalent stiffness, it will contribute allow a reduction in connection materials while accommodating the constraints in transportation. In this study, a new joint system to connect narrow width CLT panels laterally together is proposed. An experimental study was conducted to evaluate the structural performance of the proposed joint system.

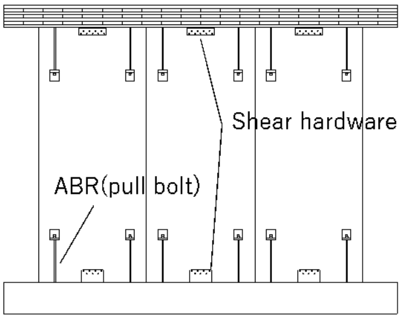

(a) typical joint system

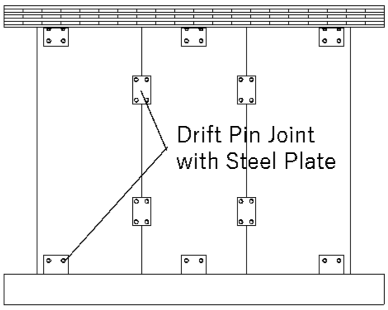

(b) proposed joint system

Fig. 1 – Comparison between the typical and proposed joint systems of CLT panels.

2. Outline of Proposed Joint

Figure 1(a) indicates the typical current CLT panel arrangement configuration that uses only floor-to-wall connections. In this construction method each CLT panel behaves independently as a single wall without any interaction with the other adjacent panels. These floor-to-wall connections are installed at the top and bottom four corners of each CLT panel in order to resist the rotational and translational deformation of a panel. For this reason, the amount of metal floor-to-wall joint elements increases, which leads to an increase in labour work and construction cost, which subsequently inhibits wide adoption of CLT construction. Therefore, in this study, a wall-to-wall connection system is proposed, in which adjacent CLT panels are connected to each other to form single large CLT wall.

In the proposed wall-to-wall joint, shown in Fig. 2(a), two steel plates are used to splice adjacent walls together, and are attached using four drift pins that are inserted through each CLT panel. All the drift pins are hollow pipes tapped with a thread, in which high tension bolts are inserted to fix the plates. When horizontal force act on a wall as shown in Fig. 2(a), shear is transferred between CLT panels through the joints, and tension and compression are taken by connections in upper and lower corners of the panel. As shown in Fig. 2(b), in a shear joint, diagonal tension and compression between drift pins transfer the shear force between panels, and vertical tension resists tension in the lower joints. When shear displacement occurs between the adjacent panels as seen in Fig. 2(b) (blue arrows), a reaction force is generated from drift pins to CLT panel via steel plate. In the authors' previous research [1], two types of failure mechanisms were observed in a CLT panel with this kind of joint system: ductile bearing failure (red in Fig. 3) in case of enough embedded length shown in Fig. 2(c), and brittle shear failure (blue in Fig. 3) in case of shorter embedded length. Type of failure and ultimate strength can be estimated from CLT panel material strength and length of embedment and pin diameter.

In this study, following three types of experiments were performed to verify the structural performance of the proposed joint system and develop structural design method:

(1) Pull-out test on a single drift pin embedded in a CLT panel to evaluate strength and failure characteristics.

(2) Cyclic loading test of proposed joint sub-assembly consisting of steel plate and four drift pins.

(3) Horizontal loading test of a pair of CLT panels connected using the proposed joint system to evaluate the global behaviour of the spliced CLT wall.

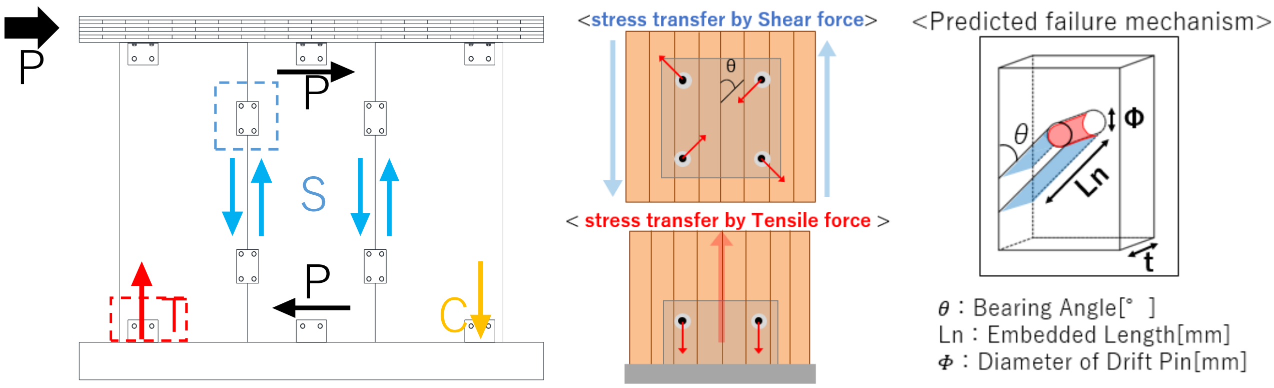

(a) Proposed joint system (b) Mechanism (c) Details of hole location

Fig. 2 – Shear transfer mechanism of the proposed joint system with steel plates and drift pins.

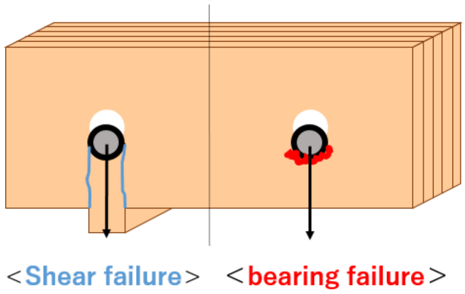

Fig. 3 – Failure mechanisms of a single drift pin.

3. Experiment on Load-carrying Capacity of a Single Drift Pin in a CLT Panel

3.1 Specimens and loading set up

A tensile test series was carried out on a single drift pin that was installed in a CLT panel. Two failure mechanisms were expected as shown in Fig. 3. Based on these test results the tensile strength of a single drift pin installed in a CLT panel is calculated using Eq. (1) - (3).

$$T = \min (Q_s, Q_{cv}) \tag{1}$$

$$Q_s = \tau \cdot L_n \cdot t \tag{2}$$

$$Q_{cv} = \sigma_{cv} \cdot \phi \cdot t \tag{3}$$

Where, Q_s and Q_{cv} are the shear strength and bearing strength of the drift pin-CLT assembly, respectively; τ and σ_{cv} is the shear and bearing stress capacity of the CLT panel, respectively; t is the CLT panel thickness, L_n is the embedded length and ϕ is the diameter of the drift pin as defined in Fig. 2(c).

In this study, L_n / ϕ = 2.5 is expected to be the boundary between the shear and bearing failure mechanisms. Therefore, when L_n / ϕ is less than 2.5 shear failure is expected as shown in Fig. 3, while when L_n / ϕ is greater than 2.5 a CLT bearing failure is expected. The test matrix and the specifications of the test specimens are shown in Table 1. Fig. 4(a) indicates the dimensions of the specimens and Fig. 4(b) indicates the loading set up used for the monotonic loading test performed on these specimens. The experimental parameters between the specimens were the ratio of the embedded length to drift pin diameter ratio (L_n / ϕ) and the angle θ between the loading direction and the direction of the grain in the outer layer of the CLT panel.

Table 1 – Specimens for experiment of shear capacity of drift pin.

Test specimen name	Material	Panel thickness	Diameter of drift pin	Fiber orientation angle	Embedded length	$\frac{L_n}{\Phi}$	Number of test specimens
		t [mm]	ϕ [mm]	θ	L_n [mm]		
40-C0-L50	CLT (Cedar) Mx60-5-5	150	40	0°	50	1.3	3
40-C30-L50				30°			
40-C45-L50				45°			
40-C60-L50				60°			
40-C90-L50				90°			
40-C0-L100				0°	100	2.5	
40-C30-L100				30°			
40-C45-L100				45°			
40-C60-L100				60°			
40-C90-L100				90°			
40-C0-L150				0°	150	3.8	
40-C30-L150				30°			
40-C45-L150				45°			
40-C60-L150				60°			
40-C90-L150				90°			

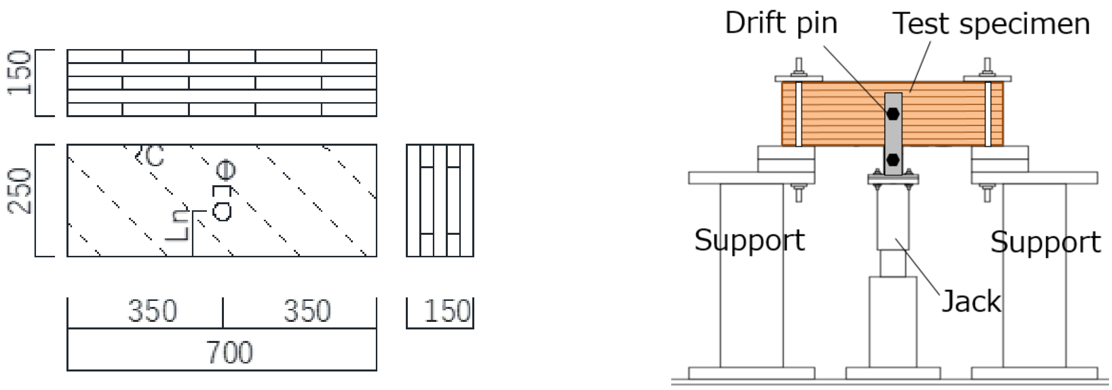

(a) Specimen

(b) Loading setup

Fig. 4 – (a) Dimensions and definintion of the specimens and loading set up.

3.2 Experimental result

The load-deformation results curves for each L_n/ϕ ratio and for each pull out angle θ are shown in Fig. 5. All specimens with $L_n/\phi = 1.3$ had shear failure with the lowest load carrying capacity comparing to other L_n/ϕ values. On the other hand, many specimens with $L_n/\phi = 3.8$ showed ductile bearing failure. In the specimens with $L_n/\phi = 2.5$, about 50% of specimens showed bearing failure while the other specimens showed shear failure. It can be said that the failure mechanism can be roughly estimated from L_n/ϕ value. As shown in Fig. 6(a), the maximum strength obtained from the tests is almost the same regardless of different values of θ angle; hence, it can be said that the influence of the fiber direction θ is almost negligible. Also, by changing the ratio L_n/ϕ, a bearing failure mechanism can be intentionally designed in order to obtain ductile joint properties. Fig. 6(b) indicates a comparison between the estimated maximum capacity calculated using Eq. (1) for different values of L_n/ϕ and the experimental values. The calculated values match the tendency of the experimental values and are generally conservative (lower) compared to the experimental values. Therefore, it is possible to roughly estimate the maximum strength of single drift pin from Eq. (1).

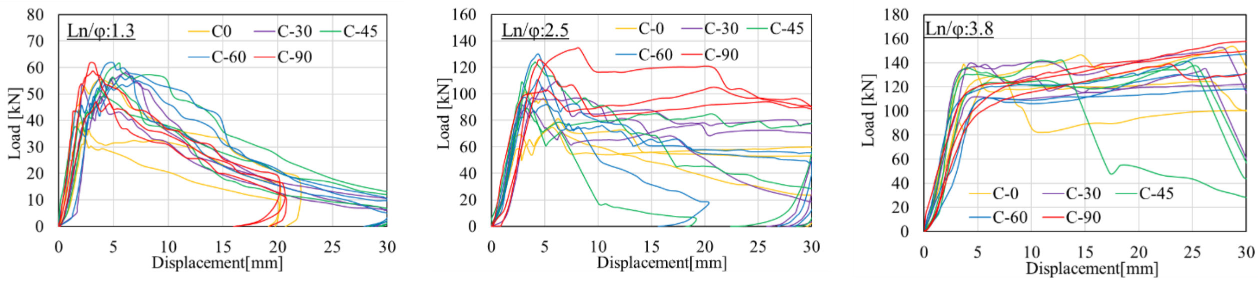

(a) $L_n/\phi = 1.3$ (b) $L_n/\phi = 2.5$ (c) $L_n/\phi = 3.8$

Fig. 5 – Load-displacement curves for all the specimens for different L_n/ϕ ratios and pull out angles, θ.

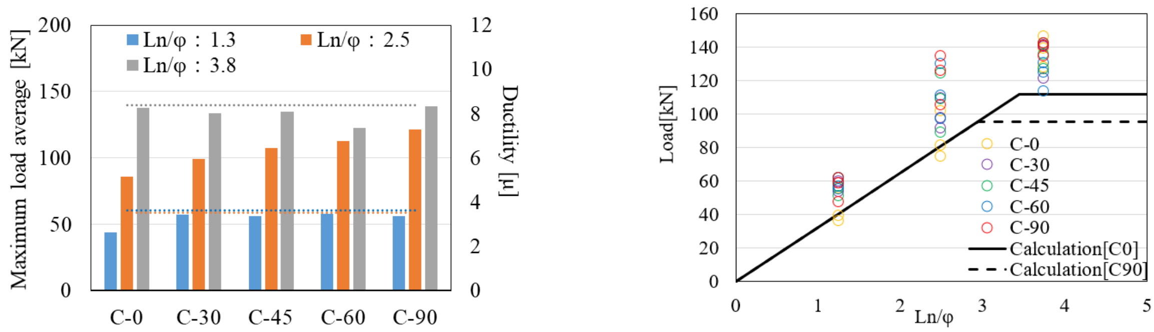

(a) Effect of loading angle relative to CLT fiber direction on the strength of the drift pin

(b) effect of L_n/ϕ ratio on load carrying capacity of the drift pin

Fig. 6 – Experimental results of pull-out strength of a single pin embedded in a CLT panel.

4. Experiment on Proposed Joint with Steel Plate and Drift Pins

4.1 Specimen and loading set up

Figure 7(a) shows the proposed wall-to-wall joint installed between CLT panels to form a single unit CLT shear wall. In this joint, two large-diameter drift pins are inserted into each CLT panel and bolted shut from both sides. Under lateral force acting of this CLT wall configuration a shear force will be generated between the two adjacent CLT panels. In order to resist this shear force, a tensile force and a compressive force are generated between the drift pin in each joint in the diagonal direction as shown in Fig. 2(c). In order to simulate this force distribution, the loading mechanism in Fig. 7(b) was proposed. The test specimen in Fig 7(b). consisted of three CLT panels connected with two steel joints. A cyclic test was conducted on this CLT specimen to obtain the shear strength of the proposed joint. The strength of the joint, R, was estimated by Eq. (4) using the tensile strength of single drift pin, T, obtained from Eq. (1) and joint angle θ that is shown in Fig. 7(b).

$$R=2*T*\cos\theta \tag{4}$$

The parameters considered in this experiment series were the embedded length L_n [mm], the drift pin diameter ϕ [mm], and the joint angle θ [°]. A total of seven different specimens were tested using this set up. The name of the test specimen consists of three parts, the first part refers to the drift pin diameter (ϕ), the second part is the angle of the joint (θ) and the last part refers to the embedded length (L_n). The test matrix and the specifications of the test specimens are shown in Table 2. The loading set up used in this experiment is shown in Fig. 8(a). The two CLT panels on each side of the specimen were fixed to the loading frame. The CLT panel in the middle was attached to an upper and lower 1000 kN loading jack, and the shear force was applied to the joint by pushing and pulling the specimen up and down using these two jacks. The specimens were tested under cyclic loading based on the loading schedule shown in Fig. 8(b). The vertical downward direction was defined as the positive direction. In this loading set up, a gap between the panels occurred at the top part of the specimen when subjected to negative loading. However, it was decided to investigate the properties of the joint when shear force and separation force simultaneously act on this joint; thus, confinement measures to suppress the opening of this gap were not taken.

The accuracy of the diameter of the hole drilled in the CLT panel was problematic due to the manual drilling method used. Therefore, the first specimen (40-θ45-L150) showed some initial slip during loading due to the gap between the drift pin and the hole in the CLT panel. In all the other specimens, epoxy adhesive was used to fill this gap before the specimen was loaded.

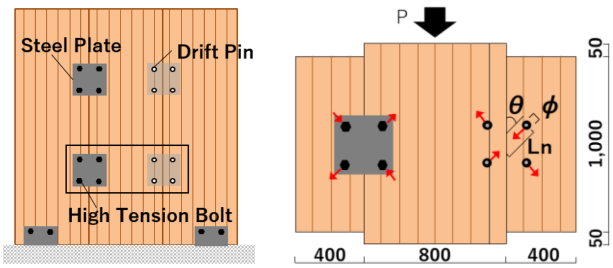

(a)

Fig. 7 – Proposed joint system and specimen for joint experiment.

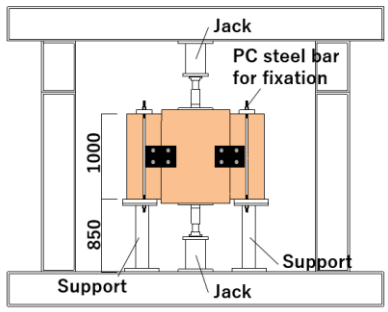

Fig. 8 – Loading set up of the joint experiment.

Table 2 – Test matrix of shear capacity for proposed joint system.

<table>
<tr><th rowspan="2">Test specimen name</th><th rowspan="2">Material</th><th>Panel thickness</th><th>Diameter of drift pin</th><th>Joint angle</th><th>Embedded length</th><th rowspan="2">L_n/ϕ</th></tr>
<tr><th>t [mm]</th><th>θ [mm]</th><th>θ [°]</th><th>Ln[mm]</th></tr>
<tr><td>40-θ30-L150</td><td rowspan="7">CLT (Cedar) Mx60-5-5</td><td rowspan="7">150</td><td rowspan="5">40</td><td>30</td><td rowspan="3">150</td><td rowspan="3">3.8</td></tr>
<tr><td>40-θ45-L150</td><td>45</td></tr>
<tr><td>40-θ60-L150</td><td>60</td></tr>
<tr><td>40-θ45-L100</td><td rowspan="4">45</td><td>100</td><td>2.5</td></tr>
<tr><td>40-θ45-L75</td><td rowspan="3">75</td><td>1.9</td></tr>
<tr><td>30-θ45-L75</td><td>30</td><td>2.5</td></tr>
<tr><td>20-θ45-L75</td><td>20</td><td>3.8</td></tr>
</table>

4.2 Experimental Results

(1) Comparison of loading behaviour and failure characteristics

Figure 9 shows the load-deformation relationship for each specimen. In the 40-θ45-L75, 30-θ 45-L75 and 40-θ45-L100 specimens, drift pins showed only a small degree of engagement with the wood, and the joint strength started to decrease due to fracture along the fiber direction of the wood surrounding the drift pins as can be seen in Fig. 9. In the other specimens, the failure mechanism was characterised by high ductility due to the bearing failure of the CLT panel, as shown in the last panel of Fig. 9. In the former case, the maximum load capacity in the negative direction of the load-deformation curve is smaller than that in the positive direction, which is considered to be due to the simultaneous effects of shear and separation forces. On the other hand, in the latter cases where the L_n / ϕ is above 2.5, the maximum strength and graph characteristics were found to be similar on both positive and negative side of the load-deformation curves. Thus, it can be said that by increasing L_n / ϕ ratio, even if the shear force and the separating force act simultaneously, the resistance against the shearing force can be sufficient in both directions.

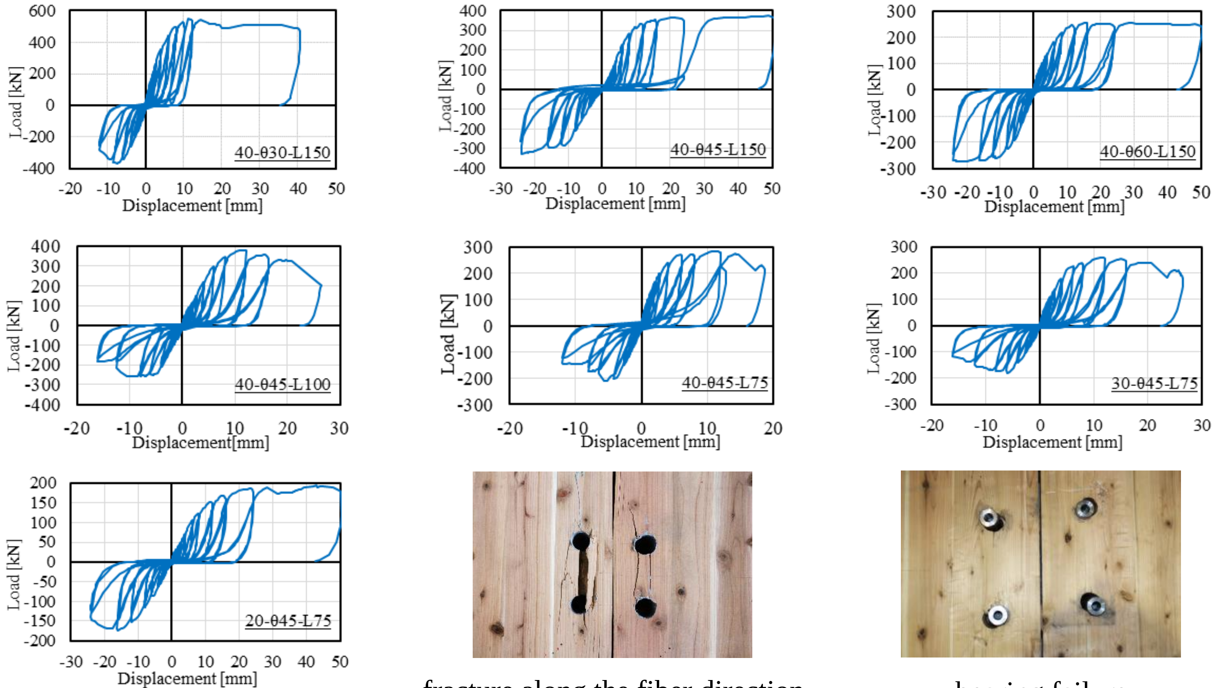

fracture along the fiber direction

bearing failure

Fig. 9 – Load-displacement curves for all the specimens and observed failure pattern.

(2) Comparison of various characteristic values

The strength, deformation and stiffness values for each specimen are summarised in Table 3. Each characteristic value was calculated by finding the bilinear curve equivalent to the backbone curve for each specimen according to the CLT Guidebook [3].

a) Effect of drift pin diameter ϕ (comparison of θ45-L75 specimens)

A comparison between backbone curves of 20-θ45-L75, 30-θ45-L75 and 40-θ45-L75 are shown in Fig. 10.a. From these results, it was confirmed that a larger the drift pin diameter results in a larger bearing area of the drift pin on the CLT panel. Therefore, the maximum strength and stiffness tend to increase. On the other hand, when the drift pin diameter is reduced, the joint tends to have a ductile CLT bearing failure and the ductility increases. In the case of bearing failure, the stiffness of the specimen decreases.

b) Effect of joint angle θ (comparison of 40-L150 specimens)

A comparison between backbone curves of 40-θ30-L150, 40-θ45-L150 and 40-θ60-L150 are shown in Fig. 10(b). From these results, it was found that by reducing the joint angle θ, the characteristic values relating to the load (P_{max}, P_y, P_u, K) tend to increase. The rate of increase can be roughly estimated by the triangular ratio cos(θ).

c) Effect of embedded length L_n (comparison of 40-θ45 specimens)

A comparison between backbone curves of 40-θ45-L75, 40-θ45-L100 and 40-θ45-L150 are shown in Fig. 10(c) From these results, it was confirmed that by increasing the embedded length L_n, the bearing failure becomes dominant and the joint strength increases. Comparing the 40-θ45-L100 specimen with the 40-θ45-L150 specimen, it can be seen that the maximum strength of both specimens was similar, but the ductility of the latter was greater.

Figure 11 illustrates a comparison between the estimated value (calculated using Eq. (4)) and the experimental value of joint strength for each specimen. The drift pin tensile strss, T, used in Eq. (4) was taken as the average maximum stress from the tensile tests in section 3.2. The calculation estimate was within 9.9% on average over all specimens, confirming that maximum strength could be roughly estimated using Eq. (4).

Table 3 – Summary of experimental results for joint shear capacity test.

Test specimen name	P_{max}	$0.8P_{max}$	P_y	P_u	$2/3P_{max}$	δ_u	δ_y	K	δ_v	$\mu=\delta_u / \delta_v$
	kN	kN	kN	kN	kN	mm	mm	kN/mm	mm	
40-θ30-L150	549.3	439.4	303.9	505.3	366.2	40.7	3.2	95.5	5.3	7.7
40-θ45-L150	373.8	299.0	273.3	360.2	249.2	51.0	7.4	37.0	9.7	5.2
40-θ60-L150	255.1	204.1	169.5	245.2	170.1	50.2	4.1	34.4	7.1	7.0
40-θ45-L100	381.9	305.5	306.9	381.2	254.6	16.4	6.7	46.0	8.3	2.0
40-θ45-L75	285.8	228.6	162.0	266.3	190.5	12.1	1.9	85.3	3.1	3.9
30-θ45-L75	260.0	208.0	153.8	241.3	173.3	22.3	3.2	47.8	5.0	4.4
20-θ45-L75	193.9	155.0	110.8	181.9	129.3	50.3	6.7	16.6	10.9	4.6

Where, P_{max}, P_y, P_u are the maximum joint strength, the yield strength and the strength at failure/termination of test, respectively. δ_u, δ_y and δ_v are the maximum displacement of the test, the yield displacement at the theoretical yield force (determined using the CLT Guidebook [3]) and the equivalent bilinear curve yield displacement, respectively. K and μ are the initial stiffness and the maximum ductility achieved in the test, respectively.

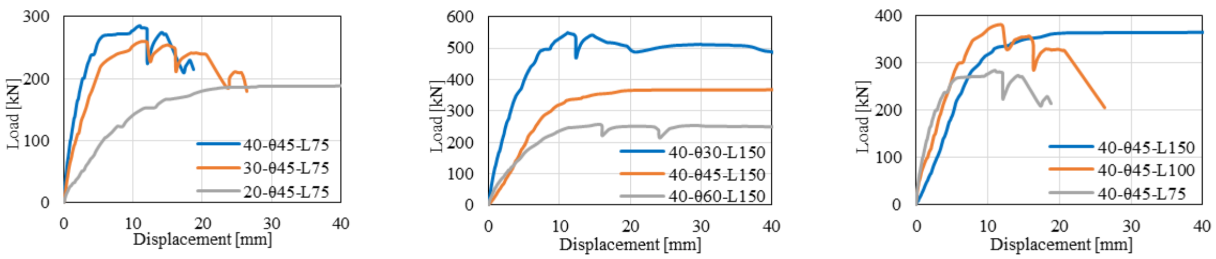

(a) Effect of drift pin diameter ϕ (b) Effect of joint angle θ (c) Effect of embedded length L_n

Fig. 10 – Backbone curves comparison.

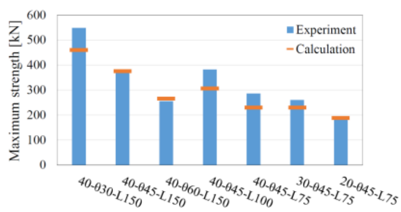

Fig. 11 – Comparison between experimental and predicted strength values.

5. Experiment on CLT wall connected by proposed joint system

In order to reduce the quantity of connection components used in conventional CLT panel wall systems, a new CLT panel connection system using the proposed joint was introduced in Fig. 1(b). The structural performance of the proposed joint was evaluated by a lateral loading test conducted on a CLT wall system utilizing the proposed joint. In the proposed CLT wall structure, shear and tensile reactions forces simultaneously act at the base-to-wall joints attached at the four corners of this wall system, and the proposed joint is used to link the narrow CLT panels.

5.1 Test matrix

In this experiment, three types of specimens were prepared as shown in Fig. 12. The objective of this experiment was to evaluate the structural performance of a two CLT panel wall system using the proposed joint method compared to a single unit CLT wall. Specimen (1) was a single unit wall, while specimen (3) was of the same dimensions as specimen (1), but consistent of two smaller panels spliced together using the proposed joint system. Specimen (2) was identical to specimen (1), but the lower wall-to-base steel angle connections were designed to yield first by providing a notch in the steel plate (50 mm x 3.2 mm) as can be seen in Fig. 12(b) and (d). As illustrated in Fig. 12, in all the tested specimens the proposed joint method was applied to the four corners of the wall as wall-to-base connections to resist shear and tensile forces simultaneously. Drift pins with M20 threaded holes at both ends and external diameter of ϕ=30 mm were used in the four corner connections. M20 high tension bolts (20 mm) was used in these wall-to-base joints to attach the drift pins to the steel plates. The foundation under all the CLT specimen was made of steel. At the top of the CLT wall there is a horizontal CLT panel that was connected to the main CLT wall using L shape connections (one at each corner of the CLT wall). In these connection, the drift pins used in the horizontal CLT panel were tapped with M12 threaded holes at both ends and had an external diameter of 20 mm ϕ=20 mm. M12 high tension bolts were used to connect all the parts together. The length of the drift pin is the same as that of the thickness of the CLT panel. Since the CLT panels comes in standard sizes, the height and width of the tested specimen were made to be half scale of the real wall, and the panel thickness was made to be the same as the thickness of the real wall. The total CLT wall width was 1200 mm and height was 1500 mm for all the specimens. The specimens used in this experiment were made with Mx 60-5-5 type (cedar) and were 150 mm thick. Specimen (1) and (3) were designed such that the CLT in the lower part of the panel (the wood surrounding the drift pins in the base of the panel) would fail in bearing, while specimen (2) was designed to fail in the notched steel plate connection.

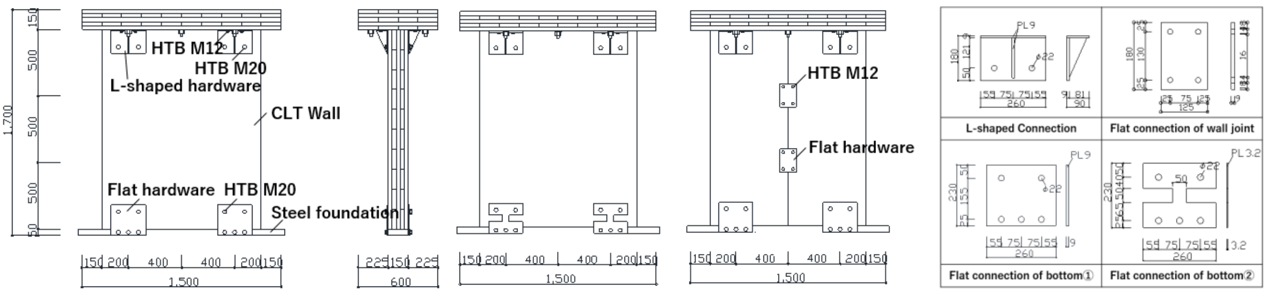

(a) specimen 1 (b) specimen 2 (c) specimen 3 (d) connection details

Fig.12 – Specimen for half scale CLT wall experiment.

5.2 Loading schedule

The loading set up is shown in Fig. 13. Regarding application of horizontal force, a shackle, wire rope, and a PC steel bar were attached to both sides of a steel plate bolted to the upper CLT component. The specimens were loaded by two centre hole jack at each side of the specimen (200 kN, stroke ± 500 mm). Before loading, a tensile force of about 5 kN was applied in advance to the right and left wire ropes in order to prevent the twisting of the specimen in the out-of-plane direction. The specimen was loaded cyclically to deformation angles of, 1/450, 1/300, 1/200, 1/150, 1/100, 1/75, 1/50, 1/33 and 1/20 rad, where the deformation angle is determined as the quotient of the horizontal displacement and the height of load application. Three cycles at each deformation angle were applied up to 1/75 rad, then two cycles up to 1/33 rad and finally one cycle at 1/20 rad.

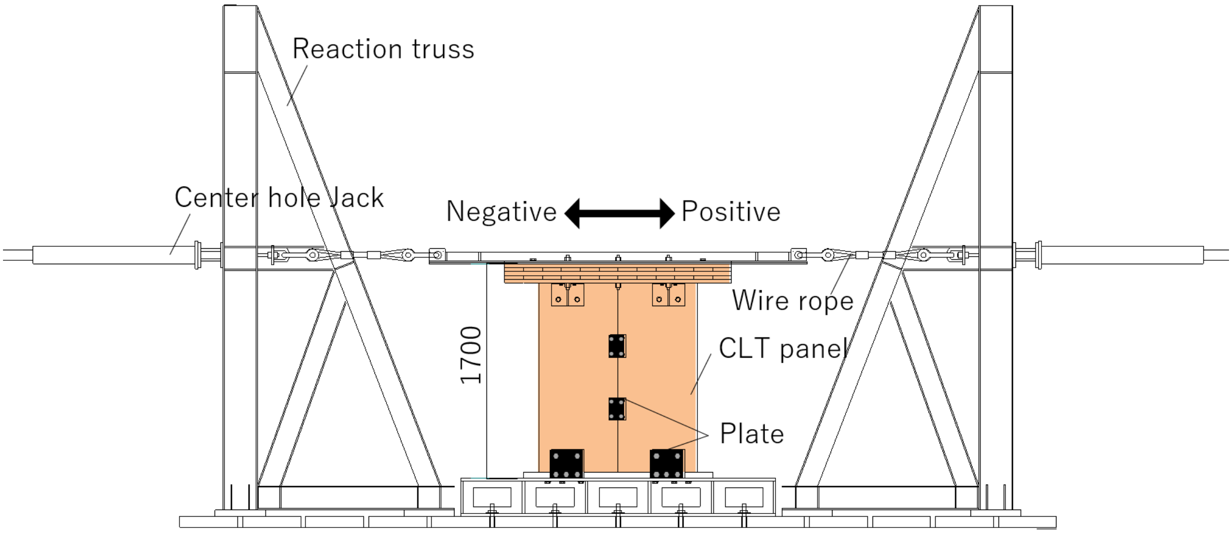

Fig. 13 – Loading setup of assembly test utilizing the proposed joint system.

5.3 Experimental results

(1) Load-deformation relationship

The relationship between the applied shear force and the deformation angle for each specimen is indicated in Fig. 14. In specimens (1) and (3), the wood yielded before the steel connections, and the strength decreased because of the failure of the wood near the deformation angle of 1/20 rad. These two specimens showed high strength characteristics at the deformation angle defined as the safety limit criterion of the design (1/30 rad). The maximum principal strain in the steel plate of the wall-to-base connections at the maximum strength reached for the wall system was about 1100 μm in both specimens. The maximum deformation between the wall panels in specimen (3) was about 8 mm, and there was no yielding in the wood or steel in the connections between the wall panels (i.e., all damage concentrated at the wall base). In test specimen (2), the notched steel plate at the wall-to-base connections yielded at 1/200 rad, and then fractured at a deformation angle of about 1/66 rad.

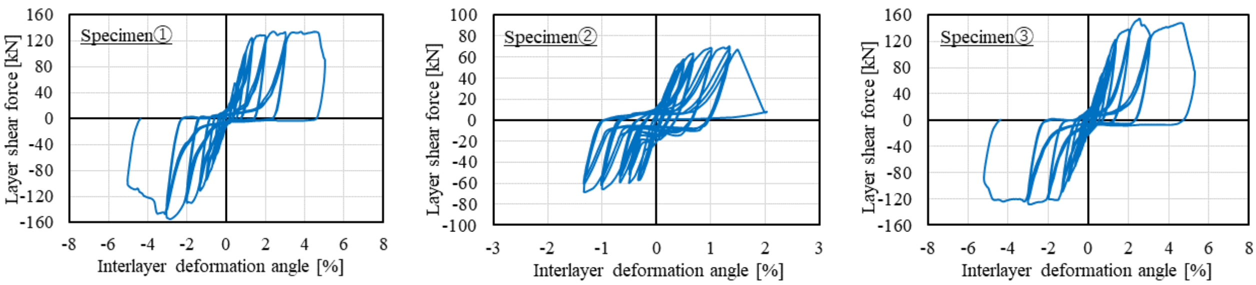

Fig. 14 – Load-displacement curves for all the assembly specimens.

(2) Failure characteristics

The failure mechanism of the wood near the wall-to-base connections of specimen (1) and (3) is shown in Fig. 15. The protrusion of the parallel layers of the CLT wall under the drift pins is due to the force applied by the pin to the CLT panel when the connection is in tension. On the other hand, CLT damage was not observed in specimen (2) as all damage concentrated in the notched steel plates at the wall-to-base connections, eventually resulting in steel fracture.

Fig. 15 – Failure pattern of the lower base-to-wall connection of specimens (1) and (3).

(3) Characteristic values

The characteristic values obtained from the experimental results are shown in Table 4. A comparison of these values between specimens (1) and (3) is shown in Fig. 16(a) Therefore, from this figure it is concluded that the wall panels spliced using the proposed joint system have the same structural performance as single unit wall of the same overall dimension.

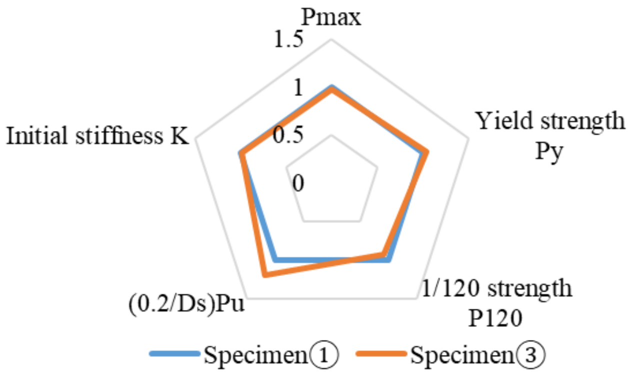

(a) Characteristics values of specimen ① and ③

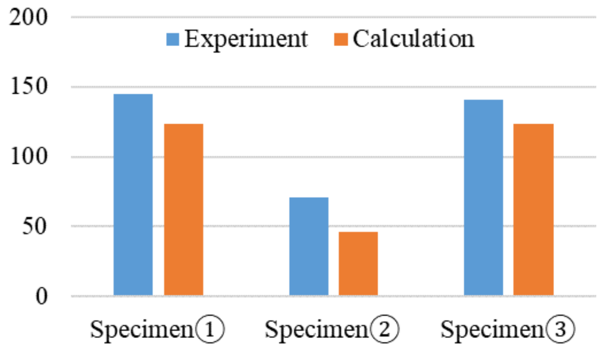

(b) Experimental strength values and calculated values for each specimen

Fig. 16 – (a) Comparison of characteristics values, experimental strength values and calculated values.

5.4 Comparison between experimental and calculated values

Figure 16(b) indicates a comparison between the experimental values obtained from this test and the calculated maximum capacity obtained by Eq. (5) that was proposed in a previous study [2]. The strength of each joint was calculated from the tested strength materials as obtained from this previous study. Compared to the experimental values, the calculated values were found to be conservative. Since specimen (2) had a different base-to-wall connection configuration (i.e., the steel plates were designed to yield first), Eq. (5) needs to be modified to consider this failure mode. One reason the calculated value was found to be less than the experimental value is that the calculation does not consider the resistance of the base-to-wall connections in the compression side of the panel. Detailed calculation methods will be examined in future.

$$FH = \frac{2 \cdot b_1}{h} \cdot FV + \frac{b_1 + b_2}{h} \cdot T_{cr} \tag{5}$$

Where, FH is shear capacity of the wall panel, FV is the vertical load acting on one panel, h is the panel height, b_0 is the length of one panel, b_1 and b_2 are the distances from the centre of the full wall assembly to the centre of the base-to-wall connections for panel 1 and panel 2, respectively and T_{cr} is maximum capacity tension of the joint.

Table 4 – Summary of experimental results for the half scale CLT wall experiment.

Test specimen name	Loading direction	P_{max}	P_y	P_u	$2/3P_{max}$	P_{120}	K	$\mu=\delta_u/\delta_v$	$(0.2/D_s)P_u$
		kN	kN	kN	kN	kN	kN/mm		kN
Specimen①	Positive	134.5	67.5	133.4	89.7	89.6	6.7	3.8	69.0
	Negative	155.5	95.4	141.7	103.7	82.2	6.2	4.8	43.5
Average		145.1	81.5	137.6	96.7	85.9	6.5	4.3	56.3
Specimen②	Positive	70.7	44.5	65.6	47.1	65.8	9.3	3.5	32.3
Specimen③	Positive	153.9	104.5	141.1	102.6	81.5	6.2	3.3	67.3
	Negative	127.7	65.0	120.3	85.1	78.1	6.6	4.3	66.6
Average		140.8	84.8	130.7	93.9	79.8	6.4	3.8	67.0

Where, P_{max}, P_y, P_u, P_{120} are the maximum strength, the yield strength, the ultimate strength (strength just before panel failure) and the strength at 1/120 rad., respectively. K and μ are the initial stiffness and the ductility, respectively.

6. Conclusions

A novel simple joint system was proposed in this study to splice multiple CLT panels together to work as a single unit. The joint consisted of steel plates at the CLT panel joints fixed with drift pins in each of the adjacent panels. The study consisted of component tests on the pull out characteristics of the drift pins, component test on the response of the joint only and full assembly tests on spliced CLT panels. The summary of the findings in this paper are as follows:

1. Regarding tensile resistance in the proposed joint method, it is possible to estimate failure characteristics and maximum strength of the single drift pin from the L_n/ϕ ratio using Eq. (1) – (3).
2. Regarding shear resistance in the proposed joint system, it is possible to estimate the maximum strength of the joint from the joint parameters using Eq. (4).
3. The CLT wall system using the proposed joint, showed high strength characteristics even at the deformation angle which corresponded to the safety limit. The strength of the wall assembly can be conservatively estimated using Eq. (5)
4. The joint wall formed by joining two narrow panels using the proposed joint method showed the same performance as a single unit wall.

7. Acknowledgements

This study was supported by the Miyagi Prefecture CLT Promotion Council. The authors are grateful to their supports.

8. References

[1] Yoshida S, Aoki K, Suzuki Y, Maeda M (2016): Development of Dovetail Joints Between Timber Panels with Large Section, *Proceedings of Annual Meeting of Architectural Institute of Japan*, Structure II, pp.141-144, 2016. 8

[2] Itoh Y, Yasumura M, Kobayashi K, Sato S (2014): Application of CLT with Local Timber Materials to Building Structures. Part 5 Cyclic Horizontal Loading Test on CLT Shear Walls, *Proceedings of Annual Meeting of Architectural Institute of Japan*, Structure II, pp.211-212, 2014. 8

[3] Japan Housing and Wood Technology Centre (2016): 2016 CLT Building Design Manual.